Supplement

Juhi Nagori et al.

In Section 1 we describe the extended model set-up, including diffusion (Section 1.1), wet deposition calculation (Section 1.2), the performance of the PATMO model for modelling isotopic sulfur (Figure S3) and the vertical profile of fractionation of the COS oxidation reactions (Figure S4). We then discuss the model performance (Section 2), the derivation of the δ budget equation (Section 3), the tropospheric budgets of SO_2 and sulfate (Table 2), and the budget profile of total S, bulk and isotopic (Section 4.1).

1 Extended Model set up

1.1 Diffusion

Equation 2 in the main text describes the turbulent eddy-driven vertical (z) mixing with K as the turbulent eddy diffusion coefficient. The profile of K in height is presented in Figure S1. These values are obtained from Massie and Hunten (1981) and multiplied by 2, in order to get enough COS oxidation in the stratosphere to match literature.

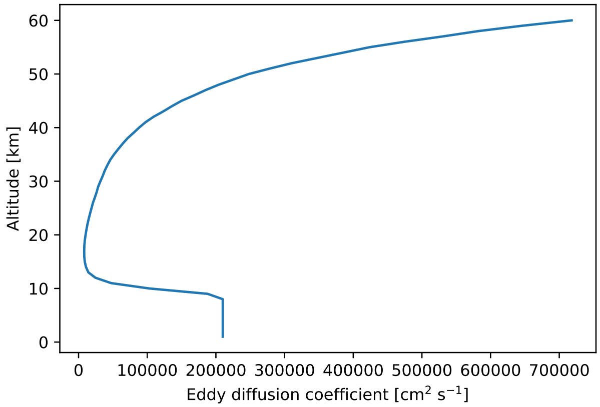

Figure S1. The turbulent eddy diffusion coefficient in height; empirical values from Massie and Hunten (1981) multiplied by 2 to match the reported COS stratospheric removal rate of 40 Gg S yr^{-1} (Brühl et al., 2012)

.

The molecular diffusion driven transport term in the model, which is part of the third term in Equation 1 of the main text, is shown below:

$$\phi_{D(i,j)} = -D_j N_j \frac{\partial f_{i,j}}{\partial z} + D_j n_{i,j} \left(\frac{1}{H_0} - \frac{1}{H_i} - \frac{\alpha_T}{T_j} \frac{dT_j}{dz} \right) \quad (1)$$

ϕ_D is in molecules cm^{-2} s^{-1}. The first part of the equation is similar to the one of eddy diffusion, depending on the D, the molecular diffusion coefficient (cm^2 s^{-1}) in layer j, N is the air density (molecules cm^{-3}) in layer j and f is the mixing ratio of the species i. The second part of the equation considers n (the number density of the molecule i in molecules cm^{-3}) and depends on the mean scale height (H_0 in cm), the molecular scale height of a molecule i (H_i in cm), the thermal diffusion factor (α_T), and the temperature T (in K) in layer j. The α_T is not considered to be important in the stratosphere (Ishidoya et al., 2013). By introducing m_a and m_i as the atmospheric average molecular mass at height z and the molecular mass of species i (in g) and by using the definition of scale height, the mass difference determines upward or downward movement (Banks and Kockarts, 2013).

$$\frac{1}{H_0} - \frac{1}{H_i} = \frac{(m_a - m_i)g}{k_B T} \qquad H_0 = \frac{k_B T}{mg} \quad (2)$$

where g is the gravitational acceleration (cm s^2) and k_B the Stefan Boltzmann constant (J K^{-1}). However, the molecular diffusion is mostly significant starting at around 100 km in the atmosphere (Hu et al., 2012) and hence is not considered in the main text.

1.2 Wet deposition

The calculation of wet deposition follows Giorgi and Chameides (1985). To calculate wet deposition Giorgi and Chameides (1985) first take into account at the amount of water and its transition time in the atmosphere. The liquid water content, the rate of removal of water in the atmosphere and the fraction of time with and without precipitation are hence considered. For each molecule the effective Henry's law or solubility constant matters, which in turn is a function of pH and temperature.

Together with these terms, and the Avogadro's constant, we calculate the removal frequency through wet deposition and we hence calculate the effective lifetime of each molecule considered. In Figure S2 the lifetime is plotted in height, and shows how fast the molecule is removed at each layer in the column model. Sulfate has the fastest wet removal: with SO_4 (purple) in the timescale of days, and H_2SO_4 (brown) in the timescale of hours. This is followed by SO_2, which ranges from days at the surface to months at 12 km. COS (blue), CS_2 (orange), H_2S (green), are very slowly rained out from the troposphere (around 10^5 years at the surface).

1.3 Zero fractionation run

To test the model, a simulation where the reaction rates for all the isotopologues are the same (a zero fractionation simulation) was carried out. The emission rates of the S isotopolgues also lead to a 0 signal, i.e. per natural abundance. Such a test is required to check whether the model is suitable for isotopologue simulations. The numerical noise of the model needs to be low enough to properly output isotopic signals. We modelled the isotopologues of S, in the current atmosphere, that were separated

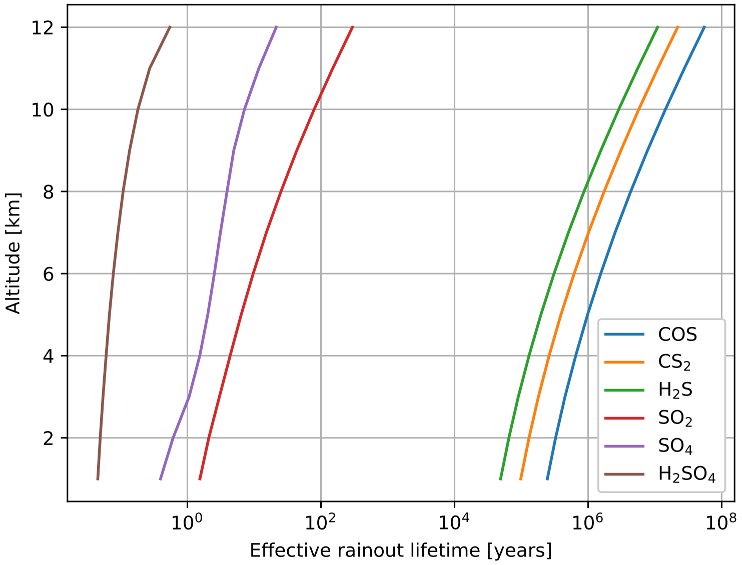

Figure S2. The effective rainout lifetime for the different S molecules, COS (blue), CS_2 (orange), H_2S (green), SO_2 (red), SO_4 (purple), and H_2SO_4 (brown).

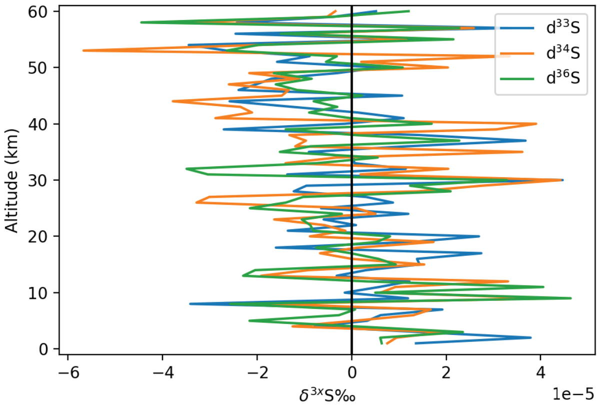

Figure S3. Zero fractionation test for Mass dependent fractionation for sulfur isotopes

per their natural abundance (VCDT). The reaction rates were the same for each isotopologue i.e. no fractionation factors were used. We observed that the numerical noise was of the order of 1e^{-5}, which is negligible compared to isotopic signals simulated in our base run in the main paper , so the model could be used for isotopic simulations.

1.4 Fractionation factors

Figure S4 shows the profiles of the fractionation factors that are used in the model for COS removal reactions: COS+OH, COS+O, and COS photolysis. The COS+OH fractionation is from Schmidt et al. (2012), due to pressure dependence this fractionation is not uniform in height. The COS+O fractionation is from Hattori et al. (2012). COS photolysis is calculated in the model. This calculation convolves the cross-sections of COS with the available radiation at different heights (see main text). The photolysis depends on shielding caused by all the species aloft, including self-shielding caused by COS.

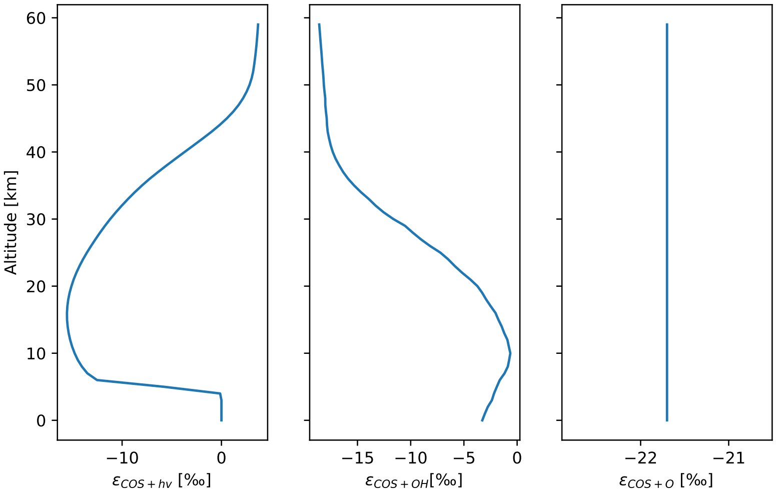

Figure S4. Height dependent ${}^{34}\epsilon$ for (a) COS + hv, (b) COS + OH and (c) COS + O^3P in ‰

2 Model performance

The model is run until steady state. To confirm that steady state is reached, we check if the total S concentration and the corresponding δ^{34}S become constant in time. First, we checked all the main sulfur molecules, for which we ran the model for 60 years. We present the vertical profiles of COS, SO_2, sulfate (here split into gas-phase H_2SO_4 and aerosol-phase SO_4) and total S in Figure S5. The mixing ratios are shown at the end of the simulation i.e. 60 years (blue line). The total S (molecules cm^3) in the atmosphere is then calculated and plotted in time (red), which reaches a steady state in less than 20 years.

We then ran the model for 60 years to check the steady state for the δ^{34}S. In Figure S6, the first plot shows the δ^{34}S in 10 year intervals and at the end of the run (orange line). The δ^{34}S in time was then plotted for different altitudes. We observe that in less than 20 years the δ^{34}S at all the different altitudes reach steady state. It is also be observed that the δ^{34}S of all the S in height does not become well mixed, which can be attributed to gravitational settling in the stratosphere, this is further discussed below.

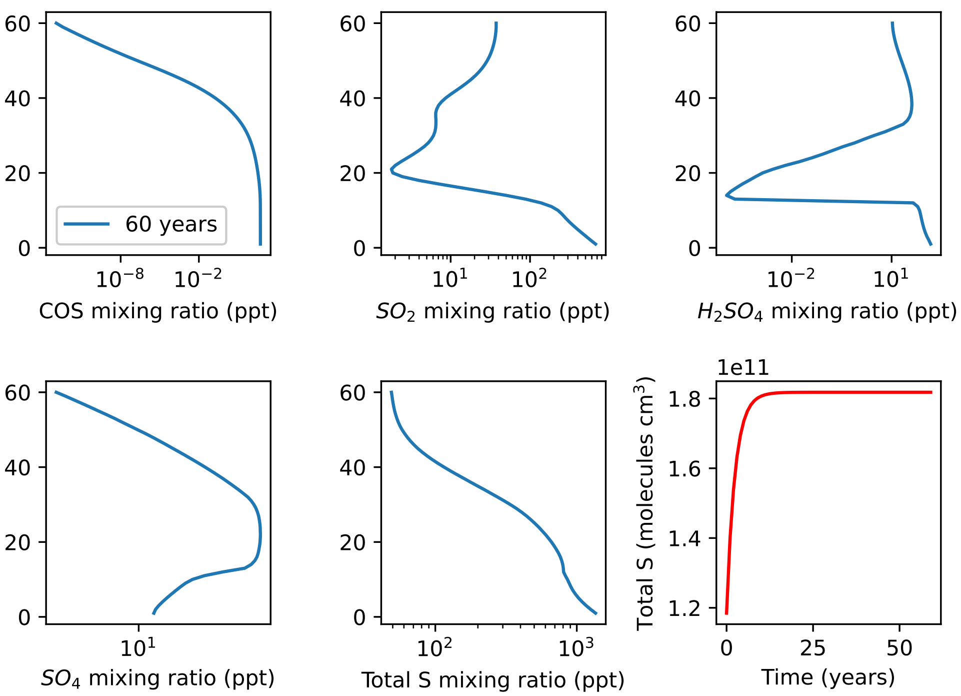

Figure S5. Results of a 60 years simulation to check whether the mixing ratios of the different sulfur gases in our model reach steady state. The bottom right panel shows the mass of S.

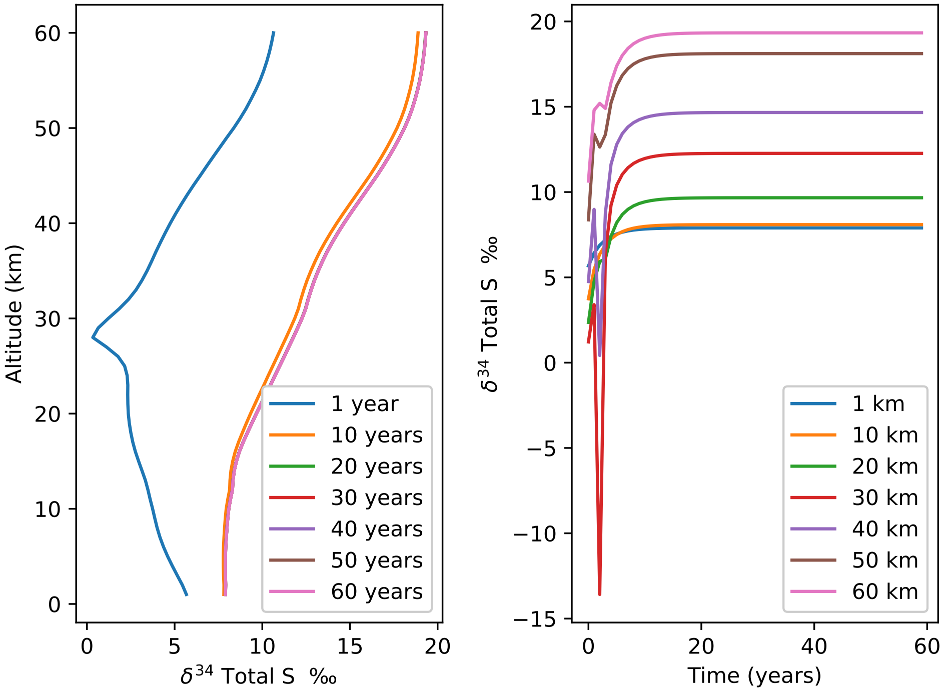

Figure S6. Results of a simulation of 60 years to check whether the δ in our model reaches steady state. In the left panel shows the δ values as a function of height for each year, while the right-hand panel shows the δ at each height as a function of time.

3 Budget equation derivation

Using the steady state approximation, we calculate the sulfur budget. The bulk sulfur budget equation depends on the following processes: Emission, Chemical production, first order loss, and transport as seen in equation 8 in the main paper. Using the same steady state approximation we derive a δ budget equation. The δ budget also has contributions from the aforementioned processes, as discussed in the main text (Equation 9) and shown here again.

$$\frac{d}{dt}\delta_A = 0 = \overbrace{(\delta_E - \delta_A)\frac{^{32}E}{^{32}C_A}}^{\text{Emission}} + \overbrace{(\alpha_y\alpha_k(\delta_{pre}+1) - (\delta_A+1))\frac{^{32}P}{^{32}C_A}}^{\text{Chemical Production}} + \overbrace{(\delta_A+1)^{32}L(1-\alpha_l)}^{\text{First Order Loss}} + \overbrace{k_t(\delta_n - \delta_A)\frac{^{32}C_n}{^{32}C_A}}^{\text{Transport}}. \tag{3}$$

In this section, we will present the derivation for all the different terms that contribute to the δ budget. The table below shows the definitions used in following derivation. While we use molecules cm^{-3}, s^{-1} and the δ notation for the derivation, to analyse the contributions in the main text, we convert the concentrations to Tg S or Gg S and the timescales to yr^{-1}.

Table 1. Definitions used in the derivation for the δ budget equation.

Symbol	Definition	Units
^{32}C	Concentration of ^{32}S molecule	molecules cm^{-3}
^{34}C	Concentration of ^{34}S molecule	molecules cm^{-3}
R	Ratio $\frac{^{34}C}{^{32}C}$	–
R$_s$	Standard ratio VCDT*	–
^{32,34}E	Emission flux	molecules cm^{-3} s^{-1}
δ	$\frac{R}{R_s}-1$	–
δ_A	δ of the atmospheric layer	–
^{32,34}L	Loss rate	s^{-1}
α	Fractionation factor $\frac{^{34}k}{^{32}k}$	-
α_l	Fractionation factor for loss rate $\frac{^{34}L}{^{32}L}$	-
α_y	Fractionation factor for yield $\frac{^{34}y}{^{32}y}$	-
^{32,34}P	Chemical production flux	molecules cm^{-3} s^{-1}
K	Eddy diffusion coefficient	cm^{2} s^{-1}
k$_t$	transport timescale = $\frac{K}{\Delta z^2}$	s^{-1}
N	Air density	molecules cm^{-3}
f	Mixing ratio	-
^{32,34}C$_a$	Concentration in atmospheric layer	molecules cm^{-3}
^{32,34}C$_n$	Concentration in neighbouring layer	molecules cm^{-3}
R$_a$	Ratio in atmospheric layer	–
R$_n$	Ratio in neighbouring layer	–

*Vienna Canyon Diablo Triolite

3.1 Emission

Firstly, we focus on the emission component of the budget equation. For this derivation, we consider that the concentration of both isotopologues is only driven by emission.

Step 1: Ratio change in time

5 The change of concentration for both isotopologues in time is described as follows:

$$\frac{d^{32}C}{dt} = {}^{32}E \qquad \frac{d^{34}C}{dt} = {}^{34}E \tag{4}$$

Using the ratio definition R, we first address at the change in ratio in time as done in Tans et al. (1993):

$$\frac{d\,^{34}C}{dt} = \frac{dR\,^{32}C}{dt} = {}^{32}C\frac{dR}{dt} + R\frac{d\,^{32}C}{dt} \qquad \therefore\ {}^{32}C\frac{dR}{dt} = \frac{d\,^{34}C}{dt} - R\frac{d\,^{32}C}{dt} \tag{5}$$

Hence for emission, the change in ratio, R, in time is multiplied with $\frac{^{32}E}{^{32}E}$ (=1) and written as:

$$^{32}C\frac{dR}{dt} = (\,^{34}E - R\,^{32}E)\frac{^{32}E}{^{32}E} \tag{6}$$

Step 2: Introducing δ definitions

Using the δ notation, we describe a δ_A, and δ_E (the δ at emission):

$$(\delta_A + 1)R_s = R \qquad (\delta_E + 1)R_s = \frac{^{34}E}{^{32}E} \tag{7}$$

Substituting Equation (7) in Equation (6) the ratio change in time becomes:

$$^{32}C\frac{dR}{dt} = ((\delta_E + 1)R_s - (\delta_A + 1)R_s)\,^{32}ER_s \tag{8}$$

Step 3: δ change in time

Finally we convert from ratio to δ notation:

using $$\delta = \frac{R}{R_s} - 1 \qquad \frac{d\delta}{dt} = \frac{1}{R_s}\frac{dR}{dt} \tag{9}$$

The final δ_A equation for emission thus becomes:

$$\frac{d\delta_A}{dt} = (\delta_E - \delta_A)\frac{^{32}E}{^{32}C_A} \tag{10}$$

The emission term therefore depends on the difference between δ at emission and the atmospheric δ, normalized by $\frac{E}{C_A}$ of the most abundant species.

3.2 Chemical Production

We next consider chemical production, and in this case we use the example of COS chemical production from CS_2 to better understand this term.

Step 1: Ratio change in time

The chemical production flux for both the isotopologues is described as:

$$^{34}P = +^{34}k^{34}C_{CS2} \qquad ^{32}P = +^{32}k^{32}C_{CS2} \tag{11}$$

Using Equation (11) and Equation (5), we describe the ratio change in time as:

$$^{32}C_{COS}\frac{dR_{COS}}{dt} = \,^{34}k^{34}C_{CS2} - R_{COS}\,^{32}k^{32}C_{CS2} \tag{12}$$

Since there are concentrations of two different S gases, we specify with a subscript which concentration belongs to which S gas. As CS_2 is the precursor gas to COS, we replace C_{CS2} with C_{pre}, while C_A and R_A represent the atmospheric concentration and ratio of COS, respectively. The ratio of precursor gas is then inserted:

$$^{32}C_A\frac{dR_A}{dt} = \,^{34}k^{32}C_{pre}R_{pre} - R_A\,^{32}k^{32}C_{pre} \qquad R_{pre} = \frac{^{34}C_{pre}}{^{32}C_{pre}} \tag{13}$$

Step 2: Introducing α definition

Using the fractionation factor α_k for the 2 reaction rates:

$$^{32}C_A \frac{dR_A}{dt} = \alpha_k\, {}^{32}k^{32}C_{pre}R_{pre} - R_A\, {}^{32}k^{32}C_{pre} \qquad \alpha_k = \frac{^{34}k}{^{32}k} \tag{14}$$

$$^{32}C_A \frac{dR_A}{dt} = {}^{32}k^{32}C_{pre}(\alpha_k R_{pre} - R_A) \tag{15}$$

According to Equation (11), $^{32}k^{32}C_{pre}$ = ^{32}P, which is the flux of ^{32}COS produced. For simplicity, we use ^{32}P to refer to this term henceforth.

Step 3: δ change in time

For the δ change in time, we use Equation (9) and the δ_A equation becomes:

$$\frac{d\delta_A}{dt} = \frac{^{32}P}{^{32}C_A}(\alpha_k R_{pre} - R_A)\frac{1}{R_s} \tag{16}$$

By introducing the δ definition in Equation (16), the rate of change of δ_A becomes:

$$\frac{d\delta_A}{dt} = \frac{^{32}P}{^{32}C_A}(\alpha_k(\delta_{pre}+1) - (\delta_A+1)) \tag{17}$$

While we have just described the example of COS production from CS$_2$, this equation remains true for all the other sulfur gas' production terms.

Yield consideration

In the main text we discuss that the reaction of CS$_2$ to COS has a yield (y) which may vary for the different isotopologues, therefore the production flux is described as:

$$^{32}C\frac{dR}{dt} = {}^{34}P - R\,{}^{32}P \qquad {}^{34}P = +{}^{34}y^{34}k^{34}C_{CS2} \qquad {}^{32}P = +{}^{32}y^{32}k^{32}C_{CS2} \tag{18}$$

Hence, if we consider a yield fractionation thus the δ equation is then:

$$\frac{d\delta_A}{dt} = \frac{^{32}P}{^{32}C_A}(\alpha_y\alpha_k(\delta_{pre}+1) - (\delta_A+1)) \qquad \alpha_y = \frac{^{34}y}{^{32}y} \tag{19}$$

The chemical production term depends on the fractionation of reaction rates, fractionation involving the yield, the δ of the precursor S gas and the δ_A, normalised by the production flux and concentration of the abundant gas.

3.3 First order loss

The next term we focus on is first order loss.

Step 1: Ratio change in time

We first describe the loss flux for both isotopes as:

$$\frac{d^{32}C}{dt} = -{}^{32}L^{32}C \qquad \frac{d^{34}C}{dt} = -{}^{34}L^{34}C \tag{20}$$

Using the formulation of Equation (5), the change in ratio in time for first order loss is:

$$^{32}C\tfrac{dR}{dt} = -(\,^{34}L^{34}C - R\,^{32}L^{32}C) \tag{21}$$

Next the ^{32}C is divided on both sides, leading to:

$$\frac{dR}{dt} = R(^{32}L - \,^{34}L) \tag{22}$$

The concentration falls out and we are left with the ratio and loss rates of the 2 isotopologues.

Step 2: Introducing α definition

We now introduce the ratio between the two loss rates i.e. α_l.

$$\frac{dR}{dt} = R(^{32}L - \alpha_l\,^{32}L) \qquad \text{where } \alpha_l = \frac{^{34}L}{^{32}L} \tag{23}$$

Substituting Equation (9) in Equation (23), we get the δ equation:

$$\frac{d\delta_A}{dt} = \frac{R}{R_s}\,^{32}L(1 - \alpha_l) \tag{24}$$

Step 3: δ change in time

The final equation, by inserting δ_A becomes:

$$\frac{d\delta_A}{dt} = (\delta_A + 1)\,^{32}L(1 - \alpha_l) \tag{25}$$

Therefore, the loss term depends on the atmospheric δ of the molecule, the loss rate for the abundant molecule, and the fractionation factor of the reaction.

3.4 Transport/Diffusion

In this model the transport works counter gradient, so the neighbouring layer also needs to be taken into account to address its contribution. The movement of gases between these two layers has a transport timescale associated with it, hence in this derivation the first step is to determine this timescale.

Step 1: Transport timescale

The main ordinary differential equation (ODE), Equation 1 in the main text, which shows the change in time of n, number density of of species i, as:

$$\frac{dn_{i,j}}{dt} = P_{i,j} - n_{i,j}L_{i,j} - \frac{\partial \phi_{i,j}}{\partial z} \tag{26}$$

The first two terms have already been discussed earlier; the ϕ represents the eddy diffusion term which is described as:

$$\phi_{i,j} = -KN(\frac{\partial f_{i,j}}{\partial z}) \tag{27}$$

The N is the air density and the f is the mixing ratio (n/N). K is the eddy diffusion coefficient. By substituting Equation (27) in Equation (26), the ODE thus becomes:

$$\frac{dn_{i,j}}{dt} = P_{i,j} - n_{i,j}L_{i,j} - KN(\frac{\partial f_{i,j}}{(\partial z)^2}) \tag{28}$$

The vertical flux in this ODE is rewritten as:

$$-KN(\frac{\partial f_{i,j}}{(\partial z)^2}) = -\frac{K}{\Delta z^2}Nf_{i,j} \tag{29}$$

$$k_t = \frac{K}{\Delta z^2} \tag{30}$$

Here we introduce a transport timescale, k_t (in s^{-1}), where K (eddy diffusion coefficient) is in cm^2 s^{-1}, and the z (height scale) is in cm.

Step 2: Ratio change in time

To account for the transport flux in the model, we consider transport as a flux between the atmospheric box (C_a) and the neighbouring box (C_n).

$$-k_t(C_a - C_n) \tag{31}$$

Here C = Nf, to stay consistent with the earlier derivations. Therefore, to calculate the change in ratio of that atmospheric layer, the equation becomes:

$$^{32}C_a\frac{dR_a}{dt} = -k_t(^{34}C_a -^{34}C_n) + k_tR_a(^{32}C_a -^{32}C_n) \tag{32}$$

By collecting the transport timescale outside the equation becomes:

$$^{32}C_a\frac{dR_a}{dt} = -k_t(^{34}C_a -^{34}C_n -^{32}C_aR_a +^{32}C_nR_a) \tag{33}$$

We eliminate some terms by including the definition of R_a. We are now left with the concentration of the neighbouring layer and the ratio of the atmospheric layer we are considering.

$$^{32}C_a\frac{dR_a}{dt} = -k_t(-^{34}C_n +^{32}C_nR_a) \tag{34}$$

By following the same step as in Equation (6), we get the following term:

$$^{32}C_a\frac{dR_a}{dt} = -k_t(-\frac{^{34}C_n}{^{32}C_n} + R_a)^{32}C_n \tag{35}$$

The ratio change in time for that layer is related to the difference in ratio in the neighbouring layer and the atmospheric box.

$$^{32}C_a\frac{dR_a}{dt} = -k_t(-R_n + R_a)^{32}C_n \tag{36}$$

Step 3: δ change in time

Using Equation (9), we arrive at the final equation:

$$\frac{d\delta_A}{dt} = k_t \frac{{}^{32}C_n}{{}^{32}C_A}(\delta_n - \delta_A) \tag{37}$$

The transport term of a layer is related to the transport timescale, the difference in δ of the neighbouring layer and the atmospheric box, normalised by the concentrations of the abundant isotopologue in the neighbouring layer and the atmospheric layer.

4 Tropospheric budget of SO_2 and sulfate

Here we include the tropospheric budgets of SO_2 and sulfate in Tg S yr^{-1}. As the scope of the paper is not to scrutinise the tropospheric budget of SO_2 and sulfate, we include it here for completeness. SO_2 emissions are a large part of the tropospheric budget of SO_2 (50.4 Tg S yr^{-1}), as is the amount produced in the troposphere (32.3 Tg S yr^{-1}). The majority of this is converted to sulfate (64.2 Tg S yr^{-1}). Wet and dry deposition of SO_2 is considerable as well (totalling 18.5 Tg S yr^{-1}). The transport of SO_2 above 16 km, however, is much smaller, at only 0.012 Tg S yr^{-1}.

Wet removal is extremely efficient in removing the sulfate in the troposphere (64.2 Tg S yr^{-1}). Sulfate is transported downwards (0.013 Tg S yr^{-1}) from the stratosphere as there is production of sulfate in the stratosphere. Lastly, gravitational settling brings more sulfate from the stratosphere to the troposphere (0.034 Tg S yr^{-1}).

Table 2. Sulfur tropospheric budget (below 16 km) in Teragrams Sulfur per year (Tg S yr^{-1}) for SO_2, and sulfate.

Process	Tropospheric SO_2 flux	Tropospheric sulfate flux
Chemical production	+32.292	+ 64.159
Chemical loss	– 64.159	0
Dry deposition	–10.114	0
Emission	+50.430	0
Wet deposition	–8.437	–64.206
Transport	–0.012	+0.013
Gravitational settling	0	+0.034
Balance	0	0

4.1 The total S budget in height

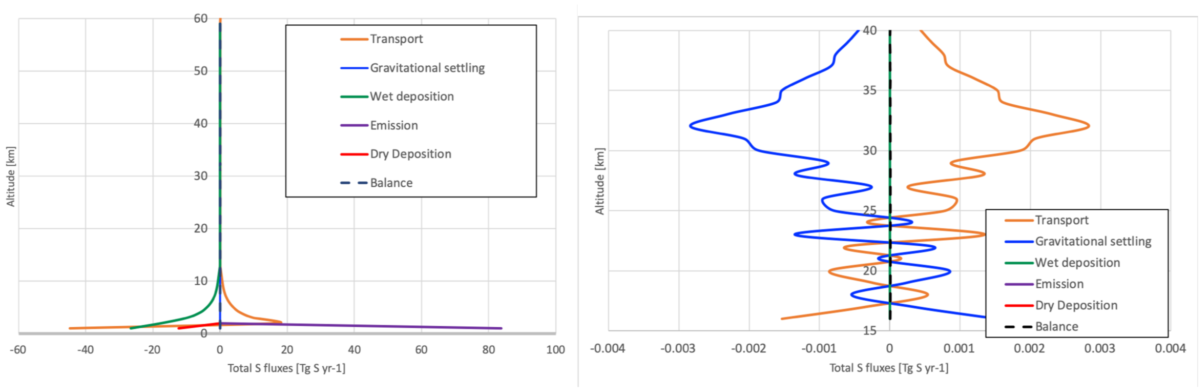

Figure S7. Total S budget. The different colours represent the different processes, and the dashed line shows the balance between these processes: net transport (orange), gravitational settling (blue), emission (purple), dry deposition (red), wet deposition (green). The left panel shows the full atmosphere, while the right panel focuses on the stratosphere (between 16–40 km), the wiggle in these profiles can be attributed to numerics.

The total S is calculated as the sum of all the sulfur species in the atmosphere. Figure S5 shows the total S and its main constituents in the model. At the surface COS and SO_2 are the major contributors to total S however, it is clear that in the rest of the troposphere COS is the main contributor to the total S. In the upper stratosphere, total S has mainly contributions from sulfate (here split into gas-phase H_2SO_4 and aerosol-phase SO4) and SO_2. The total S profiles show an accumulation of S in the Junge layer and a decrease higher up in the stratosphere. Figure S6 shows the δ profile of total S and the δ^{34}S is increasingly enriched in height. In order to understand the process that lead to this enrichment, we investigate the total S budget and the isotopic S budget in height. The total S budget (Figure S7, based on Eq. 8 in the main paper) shows the main processes that contribute to the atmospheric composition of S. Emission and dry deposition are important in the lowest model layer, with emission as the larger contributor (above 80 Tg S yr^{-1}). In the rest of the troposphere, wet deposition is balanced by the net transport. In the stratosphere, two processes matter, gravitational settling and the net transport, which work to balance each other, as the model is in steady state.

The isotopic budget shows the same processes, and their contributions. In the troposphere (Figure S8), emission accounts for introducing enriched S in the column, which is unsurprising since emission values we use for all the different S gases are introducing enriched S in the model (Table 2 in the main text). The dry deposition also enriches the atmospheric in δ^{34}S, as the lighter S is taken up preferentially due to the applied fractionation during COS dry deposition. The wet deposition profile shows that there is an enrichment of S in the higher part of the troposphere, and a depletion in the lower part. The main contributors to sulfur wet deposition are sulfate and SO_2. When we study the $\delta^{34}S$ profiles of these two gases, the $\delta^{34}S$ is depleted at the top of the troposphere compared to the lower part of the troposphere. Note here that the wet deposition does not

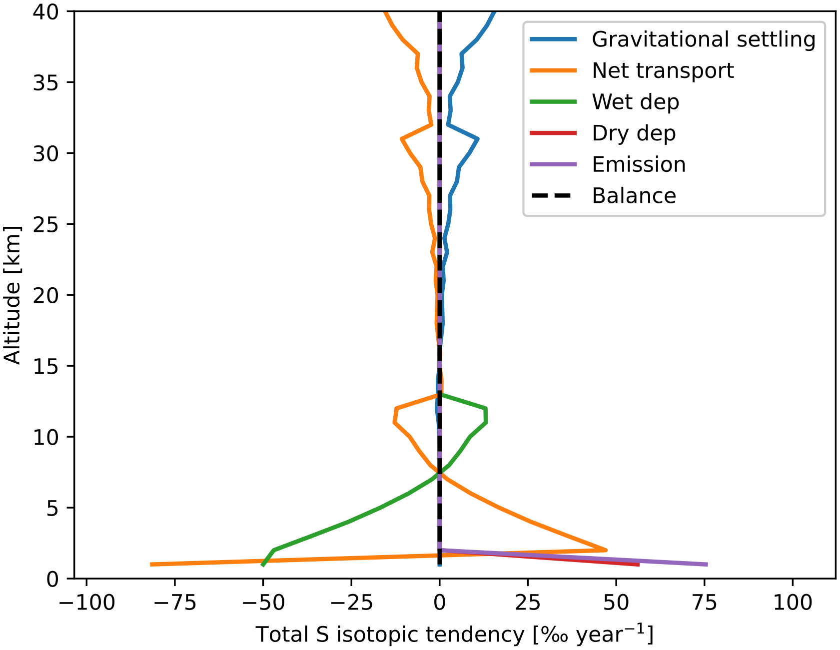

Figure S8. Stratospheric Isotopic S budget. The different colours represent the different processes, and the dashed line shows the balance between these processes: net transport (orange), gravitational settling (blue), emission (purple), dry deposition (red), wet deposition (green)

have a fractionation prescribed. As we have lighter S in the upper troposphere, the movement downwards depletes the lower troposphere. The upper troposphere is enriched as the lighter S is being lost to the lower troposphere.

When we scrutinise the the isotopic S budget in the stratosphere (Figure S9), the isotopic tendency for total S is driven by transport and gravitational settling. The gravitational settling enriches the stratosphere since it removes relatively light SO_4 ($\approx 10‰$ at 30 km, see main text, Figure 1, compared to $\approx 15‰$ for total S at 30 km (see Figure S6)). We do not prescribe a fractionation for gravitational settling; it depends on the gradient of S in each layer. In contrast, upward transport of COS depletes COS (and hence total S) because the COS gets more and more enriched towards the higher stratosphere (see Equation (37)).

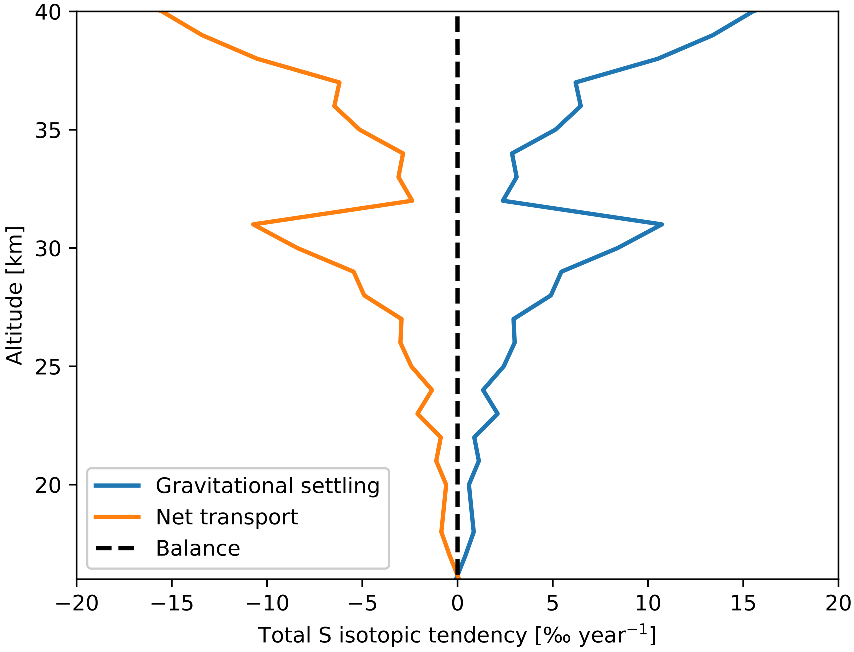

Figure S9. Stratospheric Isotopic S budget. The different colours represent the different processes, and the dashed line shows the balance between these processes: net transport (orange) and gravitational settling (blue)

4.2 No COS in the atmosphere

One of the sensitivity analysis done to highlight the importance of COS in the stratosphere involved removing COS completely from the model (See main text: Section 2.4, 3.5). In the main text we plotted the $\delta^{34}S$ of COS, SO_2 and sulfate (Figure 2), here we plot the mixing ratios of the three gases for the no COS case (blue line) versus the case with COS present (dotted black line). While a small peak in sulfate in the no COS case at 15 km is observed, there is significantly less SSA formed compared to when COS is present. Stratospheric SO_2 is also less when there is no COS in the model.

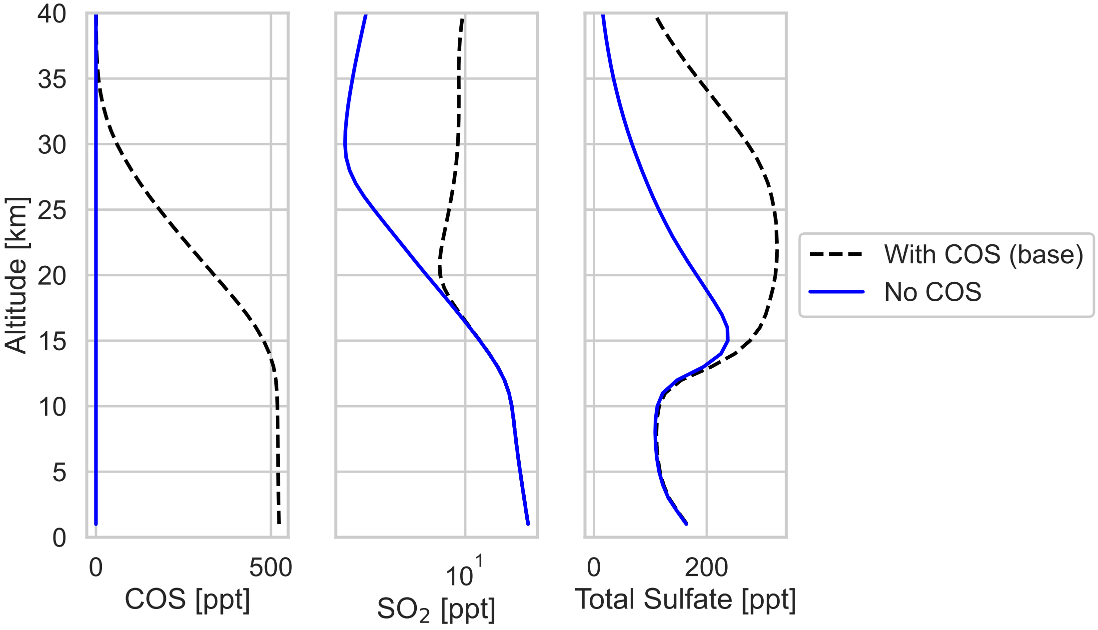

Figure S10. The mixing ratio of COS, SO_2 and sulfate with COS in the model (dotted black line) and when we remove COS from the model (blue line).

References

Banks, P. M. and Kockarts, G. (2013). *Aeronomy*. Elsevier.

Brühl, C., Lelieveld, J., Crutzen, P., Tost, H., and Stier, P. (2012). The role of carbonyl sulphide as a source of stratospheric sulphate aerosol and its impact on climate. *Atmospheric Chemistry & Physics*, 12(3).

Giorgi, F. and Chameides, W. (1985). The rainout parameterization in a photochemical model. *Journal of Geophysical Research: Atmospheres*, 90(D5):7872–7880.

Hattori, S., Schmidt, J. A., Mahler, D. W., Danielache, S. O., Johnson, M. S., and Yoshida, N. (2012). Isotope effect in the carbonyl sulfide reaction with o(3p). *The Journal of Physical Chemistry A*, 116(14):3521–3526.

Hu, R., Seager, S., and Bains, W. (2012). Photochemistry in terrestrial exoplanet atmospheres. i. photochemistry model and benchmark cases. *The Astrophysical Journal*, 761(2):166.

Ishidoya, S., Sugawara, S., Morimoto, S., Aoki, S., Nakazawa, T., Honda, H., and Murayama, S. (2013). Gravitational separation in the stratosphere–a new indicator of atmospheric circulation. *Atmospheric Chemistry and Physics*, 13(17):8787–8796.

Massie, S. and Hunten, D. (1981). Stratospheric eddy diffusion coefficients from tracer data. *Journal of Geophysical Research: Oceans*, 86(C10):9859–9868.

Schmidt, J. A., Johnson, M. S., Jung, Y., Danielache, S., Hattori, S., and Yoshida, N. (2012). Predictions of the sulfur and carbon kinetic isotope effects in the oh+ ocs reaction. *Chemical Physics Letters*, 531:64–69.

Tans, P. P., Berry, J. A., and Keeling, R. F. (1993). Oceanic 13c/12c observations: a new window on ocean co2 uptake. *Global Biogeochemical Cycles*, 7(2):353–368.